Time-Dependent Photoluminescence Spectroscopy as a Tool to Measure the Ligand Exchange Kinetics on a Quantum Dot Surface

Rolf Koole,[§†,*] Philipp Schapotschnikow,[§,‡] Celso de Mello Donegá,[†] Thijs J. H. Vlugt,[‡] and Andries Meijerink[†,*]

[†]Condensed Matter and Interfaces, Debye Institute, Utrecht University, Princetonplein 5, 3584 CC Utrecht, The Netherlands, and [‡]Process & Energy Laboratory, Delft University of Technology, Leeghwaterstraat 44, 2628 CA Delft, The Netherlands. [§]These authors have contributed equally to this work.

ABSTRACT The exchange kinetics of native ligands that passivate CdSe quantum dots (hexadecylamine (HDA), trioctylphosphine oxide (TOPO), and trioctylphosphine (TOP)) by thiols is followed *in situ*. This is realized by measuring, in real-time, the decrease in emission intensity of the QDs upon addition of hexanethiol (HT) which quenches the emission. The effect of adding an excess of native ligands prior to thiol addition on the capping exchange is studied to provide insight in the bond strength and exchange kinetics of the individual surfactants. Temperature-dependent measurements reveal faster kinetics with increasing temperature. A kinetic model to describe the time-dependent measurements is introduced, taking into account the equilibrium between native ligands before thiol addition and describing the evolution of surface coverage by all ligands over time. The model allows us to extract the quenching rate for a single thiol ligand (0.004 ns^{-1}) as well as exchange rates, equilibrium constants, activation energies, and changes in Gibbs free energy for replacement of the different native surfactants by HT. The analysis reveals that the substitution half-time of HDA by HT (72 s) is much shorter than for TOP (5 h) or TOPO (2.5 h) under the same conditions. The temperature dependence of the kinetics shows that the activation energy for exchange of HDA/TOPO by hexanethiol (1.6 kJ/mol) is much smaller than for TOP (20.9 kJ/mol).

KEYWORDS: quantum dots · ligands · exchange · spectroscopy · thiols · quenching

Surface passivation of semiconductor nanocrystals by organic ligands strongly influences the properties of these so-called quantum dots (QDs). First of all, the organic ligands control the size and shape during synthesis, by accelerating or inhibiting crystal growth at certain facets.[1,2] By varying the reaction conditions, in which the organic ligands play a dominant role, nanocrystals can now be synthesized in a wide variety of shapes such as spheres,[3,4] rods,[5−7] rings,[8] multipods,[6,7,9,10] stars and octahedrons,[8,11] cubes,[6,12] and so on. Next, stable dispersions of these colloids are a direct result of the capping molecules, avoiding irreversible aggregation and fusion of the nanocrystals due to van der Waals interactions. Most semiconductor nanocrystals are coated with hydrophobic ligands directly after synthesis, making them well soluble in apolar solvents. The nanocrystals can be transferred to more polar media such as ethanol or water by simply exchanging the hydrophobic ligands by hydrophilic or even charged ones,[4,13,14] which is a crucial step for making QDs bioapplicable.[15−17] Finally, the fluorescence of quantum dots is strongly dependent on the degree and type of surface passivation by organic ligands. For example, CdSe QDs synthesized in a trioctylphosphine/trioctylphosphine oxide (TOP/TOPO) mixture by the early synthesis route proposed by Murray *et al.* have a quantum yield (QY) of 5−15%, while the addition of hexadecylamine (HDA) to the reaction mixture, as first reported by Talapin *et al.*,[3] increases the QY to over 50% and can yield QDs with a QY near unity.[18,19] In another example closely related to the topic of this work, the fluorescence of CdSe QDs is shown to be quenched after exchanging the native ligands with thiol ligands,[20−23] while the same thiol ligands enhance the fluorescence of CdTe QDs.[24,25]

Despite the evident importance of capping molecules for both the fundamental understanding of QD properties and development toward applications, the number of detailed investigations on the surface passivation by organic ligands is limited. Early NMR and XPS studies on the surface coverage of CdSe QDs revealed that most of the surface was coated by TOPO ligands. Note that these QDs were synthesized by the early TOP/TOPO route without the presence of amines.[26,27] Other groups have utilized the influence of ligands on the

*Address correspondence to a.meijerink@uu.nl, r.koole@uu.nl.

Received for review May 28, 2008 and accepted July 22, 2008.

Published online August 12, 2008.
10.1021/nn8003247 CCC: $40.75

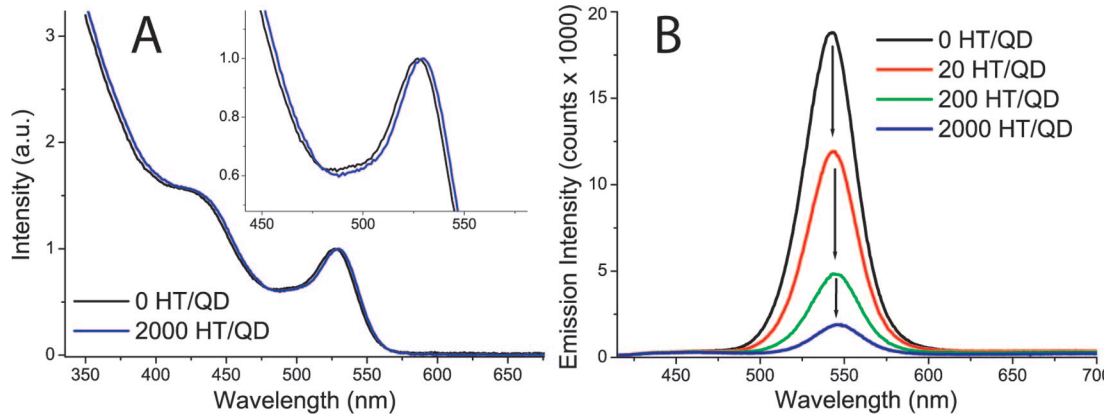

Figure 1. Absorption (A) and emission spectra (B) of CdSe QDs dispersed in toluene, after addition of a varying number of hexanethiol molecules per QD.

fluorescence properties of CdSe QDs to investigate the ligand exchange at the surface. It is generally found that primary amines enhance the QY of CdSe QDs, in particular, when the QDs have undergone several purification steps.[21−23,28,29] A quantitative study of the emission enhancement and quenching upon ligand exchange with amines and thiols, respectively, resulted in estimates for the binding constants for amines and thiols ranging between 2×10^4 and 1×10^9 M^{-1}.[21,22,29] In another study, the luminescence quenching of CdSe QDs due to thiol adsorption was shown to be significantly smaller in case the surface is mainly terminated by Se, and these Se-rich QDs required passivation using an excess of TOP to obtain a high QY (up to 50%).[30]

Molecular simulations provide another tool to study ligand adsorption. Some simulations have been performed to determine the structure of the capping layer on gold nanocrystals passivated by thiol ligands.[31−33] CdSe QDs capped by TOPO were considered by Rabani,[34] describing the surface packing and dipole moment of the cluster. Moreover, it is known from simulations of a bare CdSe QD that surface rearrangements take place to minimize the dipole moment.[34,35] Quantum chemical calculations have shown that the binding energies of amines, phosphine oxides (*e.g.*, TOPO), and acids are different for different facets, which is crucial for the size and shape control during nanocrystal growth.[36]

Previous work investigating the influence of ligand exchange on the emission of CdSe QDs focused on equilibrated samples, using steady-state measurements.[21−23] Little attention was paid to the exchange kinetics, which can be assessed by measuring the change in emission of CdSe QDs upon ligand exchange *in situ*, as is shown in this work. In a recent publication, the desorption and adsorption of alkylamines on CdSe QDs was followed over time by emission measurements.[29] The approach in that study differs from this work in the sense that the desorption kinetics of one type of ligand (amines) was studied by dilution experiments, making use of the fact that the emission intensity of CdSe QDs decreases when amine surfactants leave the surface. Breus *et al.* have recently reported a study on the ligand exchange of native ligands on CdSe/ZnS core/shell QDs by water-soluble thiolated ligands. The decrease in emission intensity as a result of this ligand exchange was studied over time, albeit with a limited number of data points with a focus on the long time regime (first data for 2 h after thiol addition).[37]

In the present work, we investigate the exchange kinetics of the three commonly used native ligands (HDA, TOP, and TOPO) on CdSe QDs by hexanethiol (HT), by measuring the decrease in emission intensity due to thiol adsorption as a function of time. The experimental conditions and time scale at which ligand exchange takes place allow us to follow the exchange process with a high accuracy and reproducibility. By changing various parameters such as native ligand concentration, hexanethiol concentration, and temperature, detailed information about the ligand exchange kinetics is extracted. A self-consistent model is developed to obtain values for reaction rates, equilibrium constants, and activation energies for ligand exchange.

This paper is divided into four sections. First, the influence of adsorbed thiol ligands on the optical properties of CdSe QDs is discussed. In this section, measurements on equilibrated samples are considered, that is, where the thiol ligands were added 3 days prior to the optical measurement. Second, we introduce a new approach to study the ligand exchange of thiols on CdSe QDs, by monitoring the emission of the QDs in real-time after addition of thiol ligands. These experiments were conducted with different concentrations of native ligands, and the results are discussed qualitatively. In the third section, a model is introduced which allows for a quantitative analysis of the results from the second part. In the last section, temperature-dependent measurements are discussed and analyzed by the same model. In this way, we obtain the activation energies and changes in Gibbs free energy for the ligand exchange of native ligands by thiols.

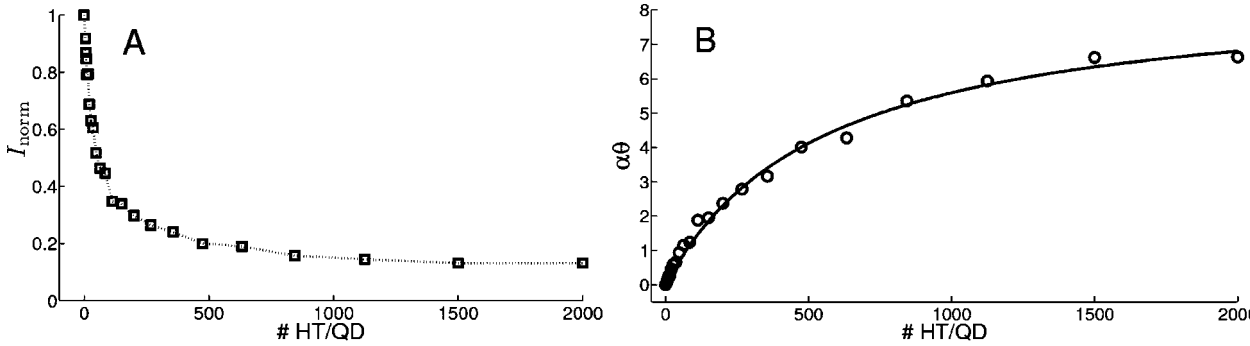

Figure 2. (A) Normalized integrated emission intensity (I_{norm}) of dispersions of CdSe QDs in toluene as a function of the number of added thiols per QD. The dotted line connecting data points serves as a guide for the eye. (B) Surface coverage (θ_{thiol}) of thiols on a QD (times a constant α), as a function of the number of thiols/QD, extracted from the data displayed in (A). Solid line is a fit of the data by a Langmuir isotherm (see eq 3), with fit parameters $\alpha = 8.7$ and $K_L = 0.0018$ [−] (corresponding to $K_L = 2600$ (mol/L)$^{-1}$ in absolute units).

RESULTS AND DISCUSSION

Equilibrium Measurements. In this section, the changes in the optical properties of CdSe QDs upon addition of hexanethiol will be discussed. In all samples described in this section, thiols were added to the QD dispersion 3 days prior to the optical measurements. This ensures that the ligand exchange had reached equilibrium, as will be shown in the next section. Figure 1A displays the absorption spectra of a dispersion of the as-synthesized CdSe QDs that were used for all experiments described throughout this paper. When an excess of effectively 2000 hexanethiol (HT) molecules per QD is added to the dispersion, a minor red shift is observed in the absorption spectrum (inset Figure 1A). We refer to an earlier publication for a detailed discussion on the origin of these small spectral changes that are observed upon addition of thiol ligands to dispersions of CdTe or CdSe QDs.[38] The emission spectrum in Figure 1B shows a narrow emission band around 542 nm (full-width at half-maximum of 36 nm, or 150 meV). The quantum yield (QY) of the QDs is high (~40%), which is in agreement with the absence of defect-related emission that is often observed at the red tail of the emission spectrum of low QY QDs. The high quality of the CdSe QDs allows for a detailed and sensitive study of the influence on the optical properties upon capping exchange with thiols. Removing an excess of ligands from the CdSe QD dispersion by (multiple) washing steps usually decreases the QY significantly (up to a factor of 10), due to the partial removal of passivating ligands. We have therefore used the as-synthesized QDs without any purification steps, which is an important difference between the present work and previous reports where ligand exchange on CdSe QDs was (quantitatively) studied.[21−23,29] In case the decrease in emission due to the adsorption of thiols is to be studied, it is beneficial to start with an as high as possible quantum yield (*i.e.*, no purification steps). On the other hand, a low QY is required (*i.e.*, multiple purification steps) in case the increase in emission intensity is monitored due to, for example, amine adsorption.[29] By using a dilution of the unpurified as-synthesized QDs, we also take advantage of the fact that the concentration of native ligands (HDA, TOP, and TOPO) is accurately known (in contrast to a dispersion of purified QDs).

Figure 1B shows the effect on the fluorescence properties of the CdSe QDs upon addition of hexanethiols in a range between 0 and 2000 HT molecules per QD. Besides a minor red shift, the emission spectra clearly show a quenching as a result of the HT addition, even at a concentration of effectively 20 HT/QD. Emission quenching of CdSe QDs as a result of the addition of thiol ligands has been studied extensively before,[21−23] and the origin of this quenching was ascribed to the trapping of photogenerated holes in the QD to a higher-lying HOMO level of thiol ligands.[25] This trapping induces an additional nonradiative recombination pathway for the exciton, resulting in a lower overall emission QY. This effect can be quantified as follows:

$$QY(\theta_{thiol}) = QY(0) \times \frac{\Gamma_{rad}}{\Gamma_{tot}} = QY(0) \times \frac{\Gamma_{rad}}{\Gamma_{rad} + N_s \cdot \theta_{thiol} \cdot \Gamma_{trap}} \quad (1)$$

where QY(0) is the quantum yield in the absence of thiols (~40%), and (Γ_{tot}) is the total decay rate of the exciton, which can be written as the sum of the radiative decay rate of the exciton (Γ_{rad}) and the total trapping rate. The total trapping rate is defined here as the trapping rate of one adsorbed thiol molecule (Γ_{trap}) times the number of adsorbed thiols, which is the product of the total number of surface sites per QD (N_s) and the surface coverage by thiols (θ_{thiol}, $0 \leq \theta_{thiol} \leq 1$). It is assumed that the trapping rate of an adsorbed thiol ligand is constant and similar for different binding sites on the QD surface. This assumption is made to limit the number of variables in the model. In practice, the quenching rate per thiol may vary between different binding sites, but this will not affect the modeling of the change in emission intensity of the ensemble of QDs.

Emission spectra as shown in Figure 1B were recorded for a large series of dispersions with HT/QD ratios ranging between 0 and 2000, again after 3 days of equilibration time. Figure 2A shows the normalized

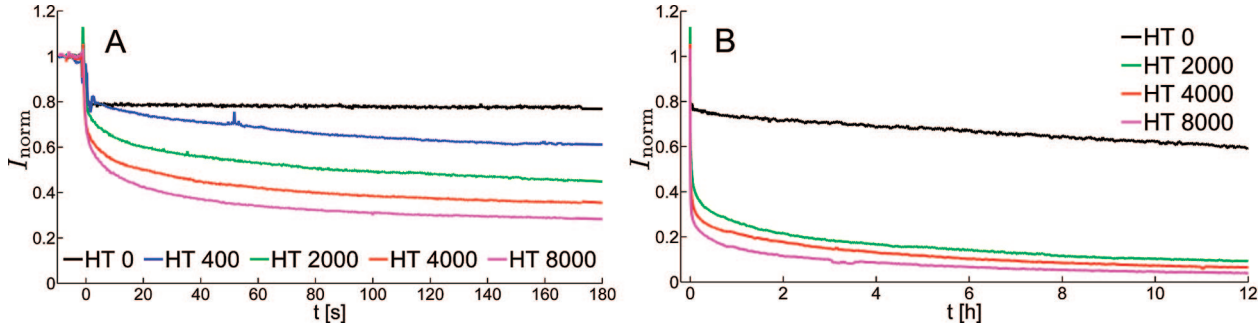

Figure 3. (A) Short time and (B) long time regime of the time-dependent decrease in emission intensity of CdSe QDs in toluene upon addition of different concentrations of thiol ligands. Reference dilution measurements (without thiols) are shown in black. All emission spectra were recorded for 0.1 s, and the normalized (to the value before injection) integrated emission intensity is plotted as a function of time.

emission intensity of the CdSe QDs as a function of the number of thiols per QD. The normalized emission intensity (I_{norm}) is defined as the integrated emission intensity of a sample, normalized to the integrated emission intensity of the dispersion without thiols (I_0). The emission intensity rapidly drops within the range of 0−100 HT/QD, after which it gradually decreases to a value of approximately 0.1. It is important for the modeling section below to translate the emission intensity into surface coverage. Normalizing and rewriting eq 1 yields

$$\alpha\theta_{thiol} = \frac{1}{I_{norm}} - 1 \qquad (2)$$

where α is a constant defined as $\alpha = N_s\Gamma_{trap}/\Gamma_{rad}$. Note that the derivation of eq 2 is similar to the derivation of the Stern−Volmer equation, which is used to describe the emission intensity of molecular emitter−quencher pairs. The data displayed in Figure 2A can now be plotted in terms of surface coverage as a function of the HT concentration (see Figure 2B). Similar to previous work,[21,22] the data can be well fitted by a Langmuir isotherm

$$\alpha\theta_{thiol} = \alpha\frac{K_L c_{thiol}}{1 + K_L c_{thiol}} \qquad (3)$$

with the effective Langmuir constant K_L. The meaning of K_L will be discussed in modeling section below. To illustrate the difference between eq 2 and the linear model used in previous work,[21,22] we compare for both methods the *titration midpoint* (*TM*): the thiol coverage at which the emission intensity is half of the total decrease in emission intensity (QY(θ_{TM}) = 0.5(QY(0) + QY(1)). If a linear relation is assumed, then $\theta_{TM} = 0.5$, whereas eq 2 yields $\theta_{TM} = 0.09$ in our case (for $\alpha = 8.7$).

The value for $\alpha\theta$ extrapolates to ~9 for infinite thiol concentration when the surface coverage by thiols (θ_{thiol}) is approximately 1 (total surface coverage). This can also be deduced by simply filling in a value of 0.1 for I_{norm} in eq 2. Assuming a total number of cadmium surface sites (N_s) of ~125 per QD (based on 0.2 nm^2 per cadmium site[29] and a particle diameter of 2.8 nm), and taking a literature value for the radiative decay rate (Γ_{rad}) of 0.05 ns^{-1} ($\tau \approx 20$ ns)[39] for CdSe QDs emitting at 540 nm, it follows that the trapping rate per thiol ligand (Γ_{trap}) is of the order of 0.004 ns^{-1}.

Time-Dependent Measurements. All experiments described above involved equilibrated dispersions of CdSe QDs to which thiols were added 3 days prior to the optical measurements. In this section, the emission intensity of the QD dispersion upon addition of thiols is followed in real-time to obtain information on the ligand exchange kinetics. This was realized by sequentially measuring the emission spectra of the CdSe QDs before, during, and after the addition of thiols. In all experiments, 0.5 mL of a toluene solution containing the desired amount of HT molecules was rapidly injected through a septum into a dispersion of ~2 nmol of CdSe QDs in 2.5 mL of toluene. In this manner, the decrease in emission intensity as a result of thiol addition could be recorded *in situ*, while the presence of oxygen was reduced to a minimum. To validate the experimental procedure, several reference experiments were conducted by injecting pure toluene (without HT) into the QD dispersion. In the short time window, this dilution was found to be highly reproducible within seconds (see Figure 3 and Figure S1A in the Supporting Information). The emission intensity decreases to 83% of the initial intensity, which is in excellent agreement with the dilution factor (2.5 mL/(2.5 mL + 0.5 mL) = 0.83). A sharp increase of 10−20% is observed at the time of injection (set to $t = -1$ s), which is ascribed to scattering of the excitation beam in the disturbed dispersion during injection. It can be seen that the injection and dilution process is very fast (1−2 s), and the subsequent emission intensity is constant over time in the short time window. These reference experiments show that the decrease in emission intensities upon thiol addition (see below) can be directly ascribed to quenching by adsorbed thiols, even on very short time scales (*viz.* seconds).

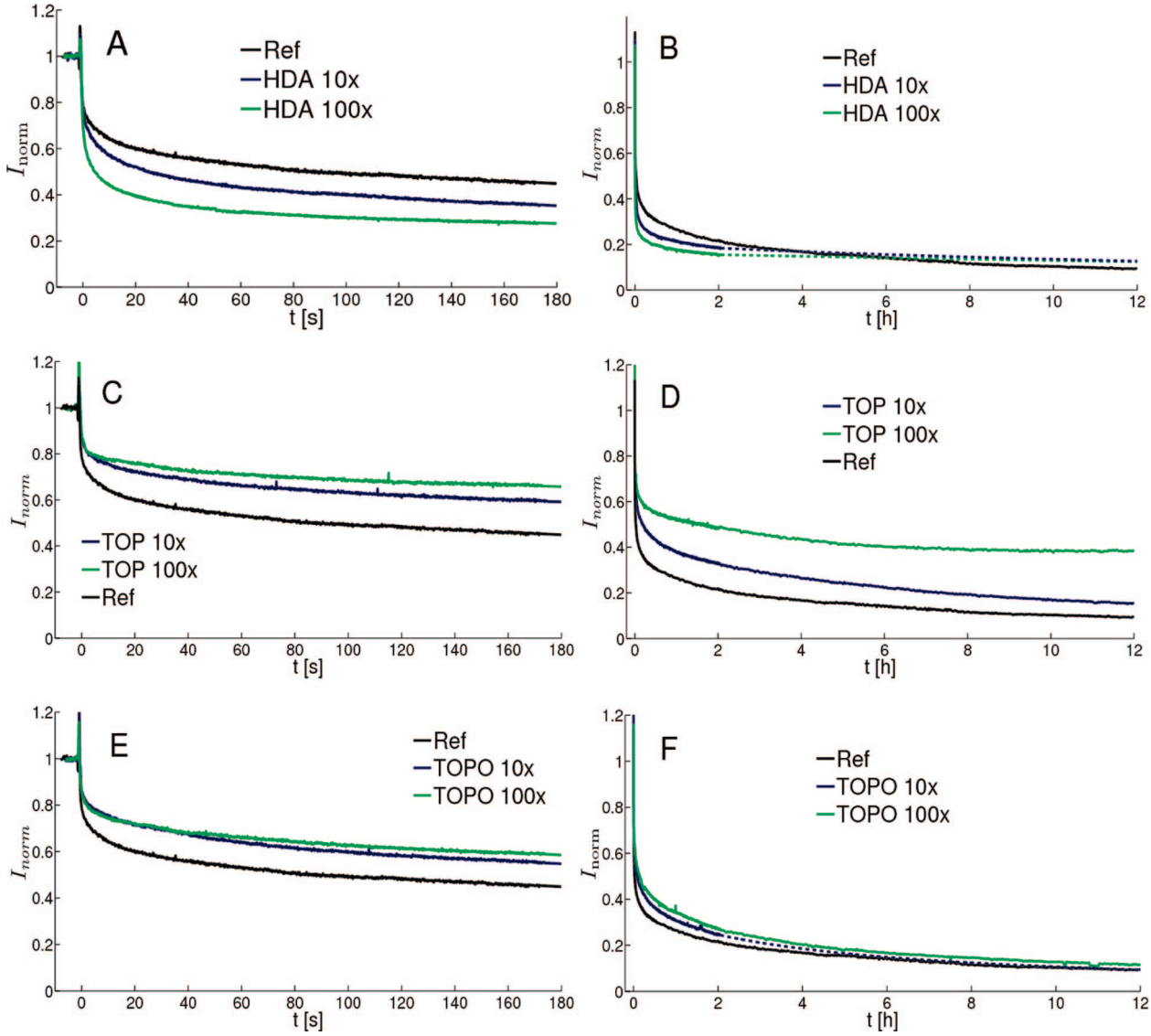

Figure 4. Time-dependent measurements of the emission intensity of CdSe QDs upon addition of 2000 HT/QD. The decrease in emission intensity for QD dispersions with a 10- or 100-fold excess of HDA (A and B), TOP (C and D), or TOPO (E and F) is compared to the standard experiment where no additional ligands were added prior to the injection of HT. Left and right panels show the evolution of the emission intensity on the short and long time scale, respectively.

The evolution of emission intensity of the CdSe QDs upon addition of thiols is plotted in Figure 3, together with the reference measurement (no thiols). Four experiments were conducted in which effectively 400, 2000, 4000, and 8000 thiols per QD were added to the dispersion. In the short time window (Figure 3A), a sharp decrease in emission intensity is observed within the first minute. In the long time regime (Figure 3B), there is still a significant decrease in emission intensity between 1 and 12 h. Clearly, the system needs at least 12 h to equilibrate. Both in the short and long time regime, it is apparent that an increase in the concentration of added thiols results in a faster and eventually larger decrease in emission intensity. The experiment of 400 HT/QD was carried out for only 30 min and is therefore omitted in Figure 3B. These experiments show that there is a very fast initial ligand exchange with the native ligands, followed by a slower process that takes up to 12 h.

The gradual decrease in emission intensity observed for the reference measurement in the long time regime (Figure 3B) may be ascribed to a slow photo-oxidation process. To investigate the possible influence of photo-oxidation in the kinetic measurements, we have performed similar experiments in the glovebox as a control or reduced the intensity of the excitation beam (by blocking the light source in between measurements). We found a similar final emission intensity for these control experiments compared to the kinetic measurements. Therefore, we ascribe the decrease in emission intensity in the long time regime predominantly to a slow adsorption process of thiols, and not to photo-oxidation. Nevertheless, it should be noted that the photo-oxidation process may slightly affect the out-

come of the quantitative analysis that is described in the modeling section below.

Figure 3 clearly shows that the ligand exchange of the native ligands of CdSe QDs by thiols is not a simple first-order process. This is not so surprising since the CdSe QDs are initially coated by a combination of ligands (HDA, TOP, and TOPO), each of which will have a different binding constant and exchange kinetics. In addition, the exchange kinetics may also be dependent on the particular facet of the nanocrystal to which a ligand is bound. Therefore, it may be expected that the replacement of the native ligands by thiols is more complex. To obtain more insight in the exchange kinetics, several experiments were carried out where an excess of one of the native ligands was present. In each case, the exchange kinetics (*i.e.*, the evolution of the emission intensity after thiol addition) was investigated after adding a 10- or 100-fold excess of one of the native ligands. The excess of ligands was added at least 3 days prior to the thiol addition, to allow the system to equilibrate. It is stressed that the addition of excess ligands did *not* influence the initial QY of the QDs, in contrast with previous reports.[21−23] This is simply because in our case the QDs were not subjected to any purification step, thereby maintaining the high QY of 40% which is not affected by the addition of excess native ligands. Figure 4 shows the decrease in emission intensity of these samples after addition of effectively 2000 HT molecules per QD, and the results are compared to the "standard" experiment where no excess ligands were added (but also 2000 HT/QD). The *in situ* measurements of 10- and 100-fold excess HDA and 10-fold excess TOPO were carried out for 2 h only. For clarity, these curves are interpolated to the end value which was measured after 12 h (dotted lines).

In case an excess of amine ligands (HDA) is present in the QD dispersion, the decrease in emission intensity is significantly faster as compared to the standard experiment, especially on the short time scale (Figure 4A). On the long time scale, it can be seen that the final emission intensity in case of an excess of HDA is slightly higher compared to the standard experiment (Figure 4B). The faster decrease in emission in the case of excess HDA is counter-intuitive because one would expect the ligand exchange by thiols to slow down in case more native ligands are present in the mixture. On the other hand, the slightly higher end value of the emission intensity after 12 h is what one would expect at a higher concentration of competing ligands. When an excess of TOP is present, the decrease in emission intensity becomes significantly slower, especially in the short time regime (Figure 4C). Remarkably, the final emission intensity is largely influenced by the TOP ligands and up to a factor of 5 higher in case of a 100-fold excess (Figure 4D). Again, these results may seem surprising because TOP coordinates to Se surface sites of the quantum dot[27] and, therefore, is not expected to directly influence the adsorption of thiols to QDs. Finally, the presence of additional TOPO slows down the ligand exchange with HT on the short time scale (Figure 4E) and results in a slightly higher end value of the emission intensity. The effects of TOPO are smaller than the effects of HDA or TOP, but in line with an intuitive ligand exchange mechanism between TOPO and HT.

The observations described above can be explained by the following qualitative model. First, TOP binds strongly to Se sites on the QD surface,[27] and because of the bulky nature of this molecule (three octyl chains pointing sideways),[21,26,40] it sterically prevents the adsorption of other ligands on neighboring surface sites. In case of a 100-fold excess of TOP, a higher coverage by TOP is expected, which reduces the number of Cd sites available for other ligands (HDA, TOPO, or HT). The smaller number of HT adsorbed on the QD surface after equilibration explains the higher emission end value in case of a 10- or 100-fold TOP excess (Figure 4D).

Further, it is clear from Figure 4a that amines are rapidly exchanged by thiols, which can be ascribed to the weaker bond strength of amines to Cd sites[41] and faster kinetics due to the relatively small surface area occupied by HDA as compared to TOP or TOPO. Addition of a 100-fold excess of amines initially causes the replacement of both TOPO and TOP by HDA during the 3 day equilibration period. Considering that the exchange rates of both TOPO and TOP by HT are much slower compared to those of amines due to their bulky size, the higher initial surface coverage by amines in case of a 10- or 100-fold HDA excess explains the faster decrease in emission intensity on a short time scale (Figure 4A). On the long time scale, however, the excess of amines naturally causes a slightly reduced equilibrium coverage of HT as compared to the standard experiment (Figure 4B). Returning to the case of an excess of TOP, the much slower decrease on the short time scale (Figure 4C) can now be explained by the replacement of HDA by TOP; the subsequent ligand exchange of TOP by thiols is much slower than the exchange of HDA by thiols. As mentioned above, this replacement of HDA by TOP is caused by the steric hindrance imposed by TOP ligands (bound to Se sites) on HDA ligands that are attached to neighboring Cd sites.

A similar reasoning holds for the slower initial decrease in emission intensity in case of prior equilibration with an excess of TOPO (Figure 4E); TOPO initially replaces the amines from the QD surface and is then slowly replaced by HT. However, the final emission intensity after 12 h in case of a 100-fold TOPO excess (Figure 4F) is much lower than that observed for an excess of TOP (Figure 4D). This indicates that the bond strength of TOP to the Se sites (hindering thiol adsorption) is larger than the TOPO−Cd bond strength and competes with thiol adsorption.

Model. In order to obtain quantitative information from the kinetic experiments described in the previous

section, a model for the ligand exchange is introduced in this section and shown to be able to explain the experimental observations. In our model, the QD surface is assumed to be completely covered with capping molecules. This does not imply that ligands are permanently bound to the surface, but that the time between desorption of a ligand and adsorption of another one is much shorter than experimental time scales. Otherwise, it would be impossible to accelerate the exchange of HT on a short time scale by increasing the concentration of another ligand (HDA). We therefore suggest a competition model consisting of three reactions

$$\mathrm{HT} + \mathrm{X}^* \underset{k_X^-}{\overset{k_X^+}{\rightleftharpoons}} \mathrm{HT}^* + \mathrm{X} \qquad (4)$$

where X denotes a native ligand (HDA, TOP, or TOPO); "$*$" describes the adsorbed state; and k_X^+ and k_X^- are the forward and backward substitution rates of X, respectively. We do not take into account the differences between surface areas occupied by a small surface area (HT, HDA) and a bulky (TOP, TOPO) ligand, and all surface sites are assumed to be equal. We also neglect the dynamics of the exchange between native ligands during the experiment. However, the model does account for the equilibrium between native ligands before thiol addition and at the end of the experiment (because they are in equilibrium with HT).

Note that the exchange of HDA or TOPO follows a different path than the exchange of TOP. In the case of HDA and TOPO, a surfactant on a cadmium site is *exchanged* by another ligand with a stronger binding headgroup, whereas TOP bound to selenium *leaves* the QD surface, creating space for an incoming thiol molecule to adsorb to an adjacent cadmium site.

The substitution constant is given by $K_X = k_X^+/k_X^-$, and large values of K_X imply a large final coverage with HT. For example, if a QD was initially coated only by the native ligand X, then K_X would be the equilibrium constant between X and HT. It is apparent from Figure 4 that k_{HDA}^+ is the largest forward rate, while K_{TOP} is the smallest substitution constant. The effective Langmuir constant in eq 3 follows directly from this model (see eq S5 in Supporting Information):

$$K_L = \frac{1}{K_{TOP}^{-1}c_{TOP} + K_{TOPO}^{-1}c_{TOPO} + K_{HDA}^{-1}c_{HDA}} \qquad (5)$$

where c_X is the concentration of the native ligand X. From the measurements in the long time regime displayed in Figure 4B,D,F, it becomes clear that TOP binds much stronger than TOPO or HDA. Therefore, the contribution of $K_{TOP}^{-1}c_{TOP}$ to the denominator of eq 5 is much larger than the other two. The value for K_L was determined to be 0.0018 from the equilibrium measurements in Figure 2B and eq 3. Thus, we obtain the first

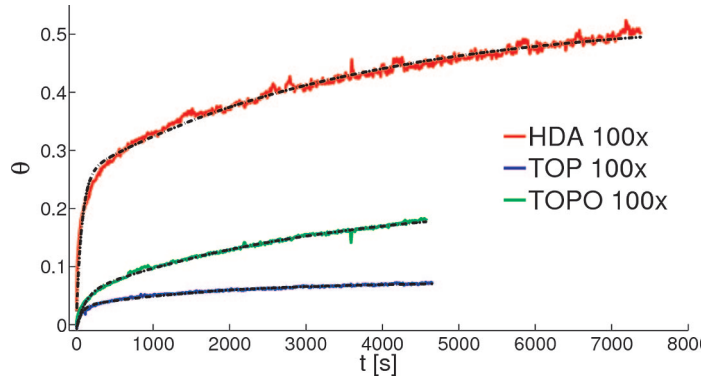

Figure 5. Fitting of the *in situ* measurements of 2000 HT/QD addition to samples with 100-fold excess (compared to concentration after synthesis) of HDA, TOP, and TOPO. Solid curves represent normalized intensities from Figure 4 transformed to coverage using eq 2 ($\alpha = 8.7$). Dashed lines represent the four-parameter fit to the model defined by eq 6.

estimate $K_{TOP} \approx K_L c_{TOP} = 2.51$ (assuming 1400 TOP molecules per QD; see Methods).

Equation 2 was used to transform the normalized intensity I_{norm} into coverage $\theta_{HT,measured}$. We have fitted the measured curves in Figure 5 to the following equation:

$$\Theta(t) = \exp(At) \cdot \Theta(0) \qquad (6)$$

where A is a matrix containing the exchange rates and concentrations of all ligands involved, defined in eq S10 in the Supporting Information, and $\Theta(t)$ is the vector containing the surface coverage by all ligands at a given time (t). The surface coverage $\Theta(0)$ before thiol injection ($t = 0$) corresponds to the equilibrium of native ligands before HT addition (see eq S9 in the Supporting Information). Equation 6 describes the collective time evolution of the surface coverage by all ligands after HT injection. Note that we can reduce the number of parameters in the model by setting the concentration of excluded components to zero. We refer to the Supporting Information for derivation of eq 6 and further details.

The fit was performed using a MATLAB script based on the deterministic derivative-free routine *fminsearch*. This routine was used to minimize the objective function

$$F(\text{rates, concentrations}) = \int_0^{t_{max}} (\theta_{HT,model}(t) - \theta_{HT,measured}(t))^2 dt \qquad (7)$$

with respect to the rate constants, where $\theta_{HT,model}(t)$ is the coverage computed using eq 6. A test for the quality of the fit is the agreement of the Langmuir constant obtained by filling in the values of the obtained substitution rate constants in eq 5, with the value for K_L obtained from Figure 2B and eq 3 ($K_L = 0.0018$). The fitting range t_{max} is set to 1.5−2 h. We did not use the full

TABLE 1. Substitution Rates and Constants and Substitution Half-Times (at 2000 HT/QD) for Different Native Ligands Obtained from Fitting the Corresponding Measurement for 100-Fold Excess of Each of the Native Ligands

X	k_X^+ [(s · mol/L)$^{-1}$]	k_X^- [(s · mol/L)$^{-1}$]	K_X [−]	$t_{1/2}$
HDA	7.5	0.017	445	72s
TOP	0.03	0.005	5.6	5.0h
TOPO	0.06	0.001	49.3	2.5h

time range for two reasons: the measurements may be affected by photo-oxidation on longer time scales, and the signal-to-noise ratio becomes worse for high HT coverage due to the lower emission intensity.

The six parameters k_X^+ and k_X^- (X = TOP, TOPO, or HDA) were fitted using eq 6 to the measured curves in three independent steps. To avoid overfitting, we only fitted four parameters in each step. The equilibrium between native surfactants before thiol injection is accounted for in eq 5 and eq S9 in the Supporting Information. During the first step, we fitted the curve with the 100-fold excess of TOP to obtain values for k_{TOP}^+ and k_{TOP}^-, while the other two rates are a combination of the exchange rates of the other ligands (TOPO, HDA) by HT. Next, we fitted the curve with the 100-fold excess of TOPO, neglecting the presence of HDA (*e.g.*, by setting its concentration to 0). However, the presence of TOP was accounted for. As a result, we obtain k_{TOPO}^+ and k_{TOPO}^-; the fitted rates for TOP are in the same order as those obtained by fitting the 100-fold TOP excess curve. Similarly, we obtained the rates for HDA, assuming no TOPO is present. Also, in this case, the rates for TOP were similar to those obtained previously. Figure 5 shows the surface coverage by HT as a function of time together with the individually fitted curves. As one can see, the latter nicely reproduce experimental data. The rates obtained from fitting can be found in the Table 1.

The values for k_X^+ support the qualitative conclusions described above: the exchange of linear amines by HT is 2 orders of magnitude faster than the exchange of branched TOP and TOPO. To illustrate the time scales, we provide *substitution half-times*

$$t_{1/2} = \frac{\ln(2)}{k_X^+ c_{HT}}$$

at the "standard" thiol concentration of 2000 HT/QD. These are the times required to replace half of the ligand X from the QD surface by HT when no other capping molecules are present and the reverse reaction does not take place. We see that while the replacement of the amine is very fast (within minutes), the replacement of branched surfactants TOP and TOPO can last hours. Interestingly, the half-time for amine replacement is close to the desorption half-time for octylamine (70 s), as was recently determined by another group.[29]

The values for K_X confirm that TOP binds stronger than HDA and TOPO and indicate that TOPO binds stronger than HDA. This suggests that the rates for HDA might even be underestimated due to TOPO present on QDs in the experiment with 100-fold amine excess, while TOPO was neglected during fitting. An estimate $K_{HDA} > 300$ (calculated as the ratio between the Langmuir constants for thiols and amines) from a previous publication[22] is in a good agreement with our value of 445. The value $K_{HDA} \approx 2$ reported by Bullen *et al.*[21] is inconsistent with our observations (Figure 3A,B) since for such a small value the replacement of HDA by thiols would be negligible in the 100-fold HDA excess measurement, which is not in line with the observed large drop in emission intensity.

We assessed the quality of the model and the fitting procedure by generating the curves using six parameters from Table 1 for the "standard" measurement where no excess ligands were present. It is important to note that these experimental data were not used for fitting and thus provide a suitable tool to test if the parameters obtained from fitting the 100-fold excess curves can reproduce the emission decay curves under "standard" conditions (no excess of native ligands). The results are shown in Figure 6. The reasonable agreement between the generated and measured curves supports the model. Deviations on the short time scale indicate that the forward substitution rate of amines is indeed underestimated, as explained above. In addition, we have fitted the experimental curve using eq 6 with all six rate constants as variables. The resulting curve fits the experimental data very well, as can be seen in Figure 6. Importantly, the values obtained for the six rate constants did not deviate more than a factor of 2 from the values listed in Table 1. This shows that the rate and equilibrium constants obtained from our model are consistent and within an acceptable accuracy.

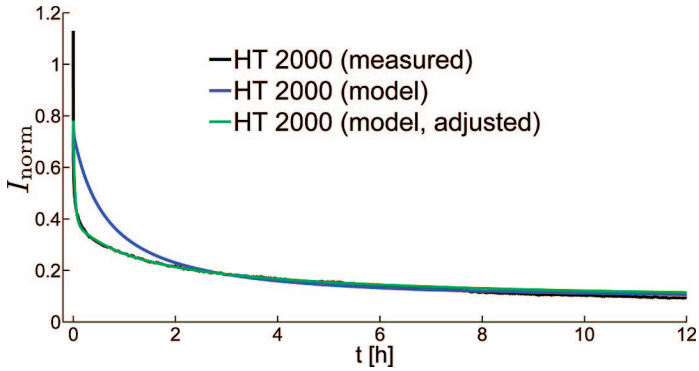

Figure 6. Time-dependent decrease in emission intensity upon thiol addition (2000 HT/QD) measured (black) and reproduced (blue and green) for the experiment without excess ligands. The blue curve was generated using the corresponding ligand concentrations and fixed rates from Table 1 and transformed into normalized intensity using eq 2. The green curve was obtained by fitting the experimental data (black) using eq 6, with all six rate constants as variables.

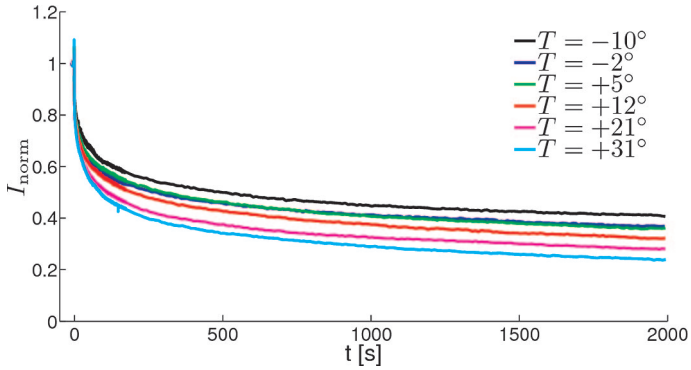

Figure 7. Time-dependent measurements of the emission intensity of CdSe QDs upon addition of 2000 HT/QD at different temperatures. All emission spectra were recorded for 0.1 s, and the normalized (to the value before injection) integrated emission intensity is plotted as a function of time.

Temperature-Dependent Measurements. To determine the activation energies for ligand adsorption and desorption, time-dependent measurements of the ligand exchange were conducted at various temperatures, by adding 2000 HT molecules per QD at $T = -10$, -2, 5, 12, 21, and 31 °C. The results are shown in Figure 7. As expected, the ligand exchange is slower for lower temperatures. The initial intensity increases with decreasing temperature from 31 to -10 °C by *ca.* 30% (not shown).

We used again eq 2 to calculate surface coverage θ from the intensity I_{norm}. Equation 1 suggests that the dominating temperature-dependent term in QY(θ) is QY(0), which cancels by normalization. Each of the curves in Figure 7 was then fitted with only four parameters to the model described in the previous section. The first rates k_X^+ and k_X^- describe the exchange of TOP ("slow" component), while the other two combine the exchange of HDA and TOPO ("fast" component). The starting parameters for the fit were created by fitting the "standard" measurement (at room temperature) on a long time scale. Because of the short time range (30 min) of the measurements, the long term properties of the system must be accounted for in a different way: the term $(K_L - K_{L,measured})^2$ was added to the objective function (eq 7). Here K_L is the Langmuir constant from eq 5, and $K_{L,measured}$ (=0.0018) is the value obtained from Figure 2B and eq 3.

The Arrhenius equation was used to relate a reaction rate k and the activation energy E_{act}:

$$k = k_0 e^{-E_{act}/RT} \quad (8)$$

where k_0 is the kinetic prefactor and R the universal gas constant. Similarly, the equilibrium constant K is related to the change in Gibbs free energy $\Delta G°$ by

$$K = e^{-\Delta G°/RT} \quad (9)$$

In Figure 8A, we plot logarithms of the four rates *versus* the inverse temperature, while Figure 8B shows the equilibrium constants. The excellent linear correlation of the data is another justification of our model and fitting procedure. Note that for the linear fits in Figure 8B the point $K_X = 1$ at infinite temperature (*i.e.*, point (0,0)) was added to the data set. However, the regression lines were not forced to go through the origin.

The activation energies E_{act} and Gibbs free energy changes $\Delta G°$ are summarized in Table 2. E_{act}^+ is the activation energy for the forward reaction, while E_{act}^- is the activation energy for the reverse reaction. It should be noted that all values lie in the order of thermal fluctuations at room temperature. The activation energy is low for the "fast" exchange of HDA/TOPO by HT. The activation energy for the reverse process can be interpreted as the energy required for removing a thiol from the QD surface, that is, the dissociation energy of a single thiol. For the exchange of TOP, E_{act} is larger than the one for HDA/TOPO, which makes it a slow process. It was discussed above that TOP binds stronger than the other native ligands, which is consistent with a higher dissociation energy. As expected, the activation energies for the exchange of HT by any of the native ligands are high since they are dominated by the dissociation of a strongly bound HT molecule. The estimate of 14−21 kJ/mol is in the same order as the one determined for binding of thiolates on CdSe QDs in aqueous solution.[42] For the exchange of a thiol by TOP, an additional con-

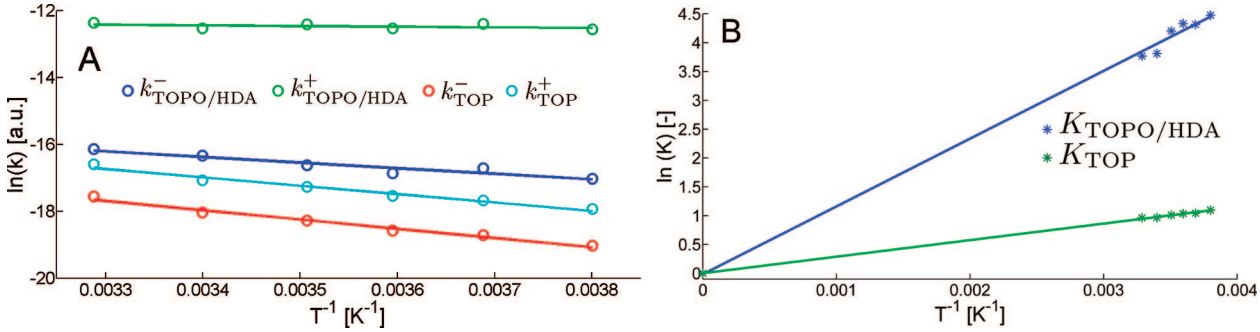

Figure 8. Arrhenius plots of the substitution rates (A) and substitution constants (B) from the temperature-dependent measurements. The point (0,0) was added to the data set in (B), to which the regression lines were fitted. Regression slopes are summarized in Table 2.

TABLE 2. Gibbs Free Energy Changes and Activation Energies the Substitution Reactions As Regression Slopes from Figure 8

X	ΔG° [kJ/mol]	E_{act}^{+} [kJ/mol]	E_{act}^{-} [kJ/mol]
HDA/TOPO	−9.9	1.6	13.9
TOP	−2.4	20.9	23.0

formational and/or surface diffusion is required (because it binds to Se sites), which may explain the higher activation energy compared to HDA/TOPO.

CONCLUSIONS

By recording the decrease in emission intensity of CdSe QDs upon addition of thiols *in situ* with a high time resolution, we were able to follow the kinetics of the ligand exchange of the native ligands (HDA, TOP, and TOPO) by hexanethiol (HT). From the relation between the emission intensity of CdSe quantum dots and the number of alkyl thiol ligands adsorbed at their surface, the surface coverage by thiols can be calculated. The quenching rate per adsorbed hexanethiol molecule was found to be 0.004 ns^{-1}. Adding an excess of HDA to the QD dispersion prior to HT injection results in faster exchange kinetics, whereas the addition of TOP or TOPO has the reverse effect. We conclude that the exchange of amines by thiols is very fast compared to TOPO. The addition of amines prior to thiol injection results in a QD surface that is predominantly covered by amines, leading to a faster overall ligand exchange. TOP binds strongly to selenium sites and sterically prevents the attachment of thiols to cadmium sites. TOP thereby slows down the ligand exchange and causes a significant shift in the equilibrium. The strong affinity of the bulky TOP molecule to the QD surface may be an important factor in controlling the growth kinetics of CdSe (and related) QDs.

The conclusions are confirmed by a kinetic model that takes into account the equilibrium between ligands before thiol addition and describes the surface coverage over time. The exchange of HDA by HT is found to be 2 orders of magnitude faster than that for TOPO or TOP. An equilibrium constant of ~500 is found for amine exchange by thiols (*i.e.*, a highly forward reaction), whereas a 10- and 100-fold smaller value is obtained for the equilibrium constants of TOPO and TOP, respectively. Temperature-dependent *in situ* measurements display slower kinetics with decreasing temperature. The data were fitted using the same model, from which the activation energies for the exchange of HDA/TOPO (1.6 kJ/mol) and TOP (20.9 kJ/mol) by thiols could be extracted. The binding energy of thiols to the QD surface is estimated to be between 14 and 23 kJ/mol. The changes in Gibbs free energy are −9.9 and −2.4 kJ/mol for the thiol exchange of HDA/TOPO and TOP, respectively. The results provide insight in binding and kinetics of ligands at the QD surface for some of the commonly used ligands for surface passivation of CdSe and CdTe QDs. In view of the prominent role of ligands on the (opto-electronic) properties and stability of QDs, the results are important for a better understanding and control in the synthesis of QDs and for tailoring their properties by ligand exchange.

METHODS

Anhydrous toluene (99.8%), trioctylphosphine (TOP, 90%), trioctylphosphine oxide (TOPO, 99%), hexadecylamine (HDA, 90%), and hexanethiol (HT, 95%) were purchased from Aldrich. Rhodamine B was supplied by Exciton. Dimethylcadmium ($Cd(Me)_2$, 99.99%) and selenium powder (99.99%, 200 mesh) were obtained from ARC Technologies and Chempur, respectively.

The synthesis of CdSe nanocrystals was carried out by the high-temperature organometallic synthesis as reported in detail by de Mello Donegá *et al.*[19] In short, a solution of the precursor materials $Cd(Me)_2$ (0.28 g) and selenium (0.79 g) in 10 mL of TOP was quickly injected into a three-neck flask containing a preheated mixture (300 °C) of 10 g of HDA and 20 g of TOPO. Upon injection, we allowed the temperature to drop to 165 °C during 5 min, followed by 6 min heating time to 240 °C, at which temperature it was kept for 4 min. After this, the reaction mixture was allowed to cool down to room temperature. The resulting CdSe QDs were 2.8 nm in diameter (as determined from TEM) and had a QY of ~40%. The QY was determined by comparison of the integrated emission intensity of a reference dye (Rhodamine B in ethanol, QY = 90%) with the emission intensity of the CdSe QDs, correcting for the absolute absorbance value at the excitation wavelength (400 nm). The raw product was diluted in a 1:1 ratio with anhydrous toluene to obtain what will be called the stock dispersion of QDs.

All samples were prepared in a nitrogen purged glovebox and transferred to a sealed quartz cuvette for optical measurements. For the equilibrium measurements, 10 μL of the stock dispersion of CdSe QDs was added to 2.5 mL of toluene, after which 0.5 mL of a solution with the desired quantity of HT in toluene was added. The samples were allowed to equilibrate for 3 days in the dark in the glovebox, after which the absorption and emission spectra were recorded. The size-dependent calibration curve of the extinction coefficient of CdSe QDs at the first absorption peak (empirically determined by Yu *et al.*[43]) was used to calculate the concentration of the QD dispersions. In this manner, we measured that the QD concentration of the samples thus obtained was ~0.7 μM (~2 nmol QDs in 3 mL of toluene). This concentration was used to compute that the 0.5 mL solution corresponding to 2000 HT molecules per QD in the final mixture requires an HT concentration of 8 mM.

For the time-dependent measurements, a dispersion of 10 μL of CdSe stock dispersion in 2.5 mL toluene was transferred (in the glovebox) into a quartz cuvette that was tightly sealed by a septum. The cuvette was placed in the sample holder of a spectrofluorometer (see below), after which 0.5 mL of an HT solution in toluene was vigorously injected with a syringe (prepared in the glovebox) through the septum of the cuvette, into the QD dispersion. A few seconds before injection of the HT solution, the recording of emission spectra was started. This was performed using a monochromator and CCD camera (see below) with a high repetition rate so that 10 emission spectra per second could be measured. During the first 3 min, the emission spectra were recorded sequentially with a repetition rate of 10 spectra per second, directly followed by 2 h (or 30 min) of measurements with a 10 s time interval, followed by a last series of measurements over 10 h with a 100 s time interval. The reference measurements (injection of 0.5 mL of toluene containing no HT) were carried out in the exact same manner. The samples con-

taining an excess of ligands were prepared by adding 10 μL of CdSe stock dispersion to 1.25 mL of toluene, to which 1.25 mL of a toluene solution containing the desired quantity of HDA, TOP, or TOPO was added. The dispersion was allowed to equilibrate for at least 3 days in the dark (in the glovebox), after which the optical measurements were started upon injection of a 0.5 mL HT solution in toluene. From the amounts used in the synthesis, it can be calculated that 10 μL of the stock dispersion of CdSe QDs contains 5 μmol HDA, 3 μmol TOP, and 6.5 μmol TOPO, which corresponds to, respectively, 2500, 1400, and 3200 ligands per QD (in the standard dispersion). These numbers were used to calculate the amount of these native ligands that was needed to obtain a 10- or 100-fold excess compared to the concentrations in the standard dispersion.

For the temperature-dependent (real-time) measurements, the sample holder of a Spex Fluorolog spectrofluorometer was replaced by a 1 L glass beaker filled with ethanol. The element of a thermostat was placed in the beaker to obtain a constant temperature, tunable between −20 and +31 °C. The cuvette was partly plunged in the ethanol and tightly fixed, and the ethanol was gently stirred for an efficient heat exchange with the cuvette, but avoiding turbulence that would cause fluctuations in the excitation/emission intensity. The syringe containing the HT solution to be injected in the QD dispersion was brought to the same temperature as the cuvette prior to injection.

Emission spectra were recorded using a 450W Xe lamp as excitation source and a double grating 0.22 m SPEX monochromator (of a SPEX Fluorolog) to select the excitation wavelength of 406 nm. Emission was collected through an optical fiber leading to a 0.3 m monochromator (150 lines/mm, blazed at 550 nm) and detected by a liquid nitrogen cooled Princeton Instruments CCD camera (1024 × 256 pixels). Absorption spectra were measured on a Perkin-Elmer Lambda 16 UV/vis spectrofluorometer.

Acknowledgment. Financial support from the European Union network "FULLSPECTRUM" (SES6-CT-2003-502620) is gratefully acknowledged by R.K. Help from D.H. van Dorp and J.G.M. Ligthart for the experimental setup is greatly appreciated. T.J.H.V. acknowledges financial support from The Netherlands Organization for Scientific Research (NWO-CW) through a VIDI grant. P.S. would like to thank the CMI group at Utrecht University for hospitality, as well as B. Hommersom for assistance in creating the TOC image.

Supporting Information Available: Reference measurements showing the emission upon diluting with pure toluene in the short and long time window, and derivations of several equations discussed in the paper are given in the Supporting Information. This material is available free of charge *via* the Internet at http://pubs.acs.org.

REFERENCES AND NOTES

1. Jun, Y. W.; Seo, J. W.; Oh, S. J.; Cheon, J. Recent Advances in the Shape Control of Inorganic Nano-Building Blocks. *Coord. Chem. Rev.* **2005**, *249*, 1766–1775.
2. Yin, Y.; Alivisatos, A. P. Colloidal Nanocrystal Synthesis and the Organic−Inorganic Interface. *Nature* **2005**, *437*, 664–670.
3. Talapin, D. V.; Rogach, A. L.; Kornowski, A.; Haase, M.; Weller, H. Highly Luminescent Monodisperse CdSe and CdSe/ZnS Nanocrystals Synthesized in a Hexadecylamine-Trioctylphosphine Oxide-Trioctylphospine Mixture. *Nano Lett.* **2001**, *1*, 207–211.
4. Murray, C. B.; Norris, D. J.; Bawendi, M. G. Synthesis and Characterization of Nearly Monodisperse CdE (E = Sulfur, Selenium, Tellurium) Semiconductor Nanocrystallites. *J. Am. Chem. Soc.* **1993**, *115*, 8706–8715.
5. Peng, X. G.; Manna, L.; Yang, W. D.; Wickham, J.; Scher, E.; Kadavanich, A.; Alivisatos, A. P. Shape Control of CdSe Nanocrystals. *Nature* **2000**, *404*, 59–61.
6. Lifshitz, E.; Bashouti, M.; Kloper, V.; Kigel, A.; Eisen, M. S.; Berger, S. Synthesis and Characterization of PbSe Quantum Wires, Multipods, Quantum Rods, and Cubes. *Nano Lett.* **2003**, *3*, 857–862.
7. Manna, L.; Scher, E. C.; Alivisatos, A. P. Synthesis of Soluble and Processable Rod-, Arrow-, Teardrop-, and Tetrapod-Shaped CdSe Nanocrystals. *J. Am. Chem. Soc.* **2000**, *122*, 12700–12706.
8. Cho, K. S.; Talapin, D. V.; Gaschler, W.; Murray, C. B. Designing PbSe Nanowires and Nanorings through Oriented Attachment of Nanoparticles. *J. Am. Chem. Soc.* **2005**, *127*, 7140–7147.
9. Peng, X. G. Mechanisms for the Shape-Control and Shape-Evolution of Colloidal Semiconductor Nanocrystals. *Adv. Mater.* **2003**, *15*, 459–463.
10. Manna, L.; Milliron, D. J.; Meisel, A.; Scher, E. C.; Alivisatos, A. P. Controlled Growth of Tetrapod-Branched Inorganic Nanocrystals. *Nat. Mater.* **2003**, *2*, 382–385.
11. Houtepen, A. J.; Koole, R.; Vanmaekelbergh, D. L.; Meeldijk, J.; Hickey, S. G. The Hidden Role of Acetate in the PbSe Nanocrystal Synthesis. *J. Am. Chem. Soc.* **2006**, *128*, 6792–6793.
12. Lu, W. G.; Fang, J. Y.; Ding, Y.; Wang, Z. L. Formation of PbSe Nanocrystals: A Growth toward Nanocubes. *J. Phys. Chem. B* **2005**, *109*, 19219–19222.
13. Wuister, S. F.; Swart, I.; van Driel, F.; Hickey, S. G.; de Mello Donegá, C. Highly Luminescent Water-Soluble CdTe Quantum Dots. *Nano Lett.* **2003**, *3*, 503–507.
14. Talapin, D. V.; Rogach, A. L.; Mekis, I.; Haubold, S.; Kornowski, A.; Haase, M.; Weller, H. Synthesis and Surface Modification of Amino-Stabilized CdSe, CdTe and InP Nanocrystals. *Colloid Surf. A* **2002**, *202*, 145–154.
15. Michalet, X.; Pinaud, F. F.; Bentolila, L. A.; Tsay, J. M.; Doose, S.; Li, J. J.; Sundaresan, G.; Wu, A. M.; Gambhir, S. S.; Weiss, S. Quantum Dots for Live Cells, *In Vivo* Imaging, and Diagnostics. *Science* **2005**, *307*, 538–544.
16. Mattoussi, H.; Mauro, J. M.; Goldman, E. R.; Anderson, G. P.; Sundar, V. C.; Mikulec, F. V.; Bawendi, M. G. Self-Assembly of CdSe-ZnS Quantum Dot Bioconjugates Using an Engineered Recombinant Protein. *J. Am. Chem. Soc.* **2000**, *122*, 12142–12150.
17. Chan, W. C.; Nie, S. Quantum Dot Bioconjugates for Ultrasensitive Nonisotopic Detection. *Science* **1998**, *281*, 2016–2018.
18. Qu, L.; Peng, X. Control of Photoluminescence Properties of CdSe Nanocrystals in Growth. *J. Am. Chem. Soc.* **2002**, *124*, 2049–2055.
19. de Mello Donegá, C.; Hickey, S. G.; Wuister, S. F.; Vanmaekelbergh, D.; Meijerink, A. Single-Step Synthesis to Control the Photoluminescence Quantum Yield and Size Dispersion of CdSe Nanocrystals. *J. Phys. Chem. B* **2003**, *107*, 489–496.
20. Kuno, M.; Lee, J. K.; Dabbousi, B. O.; Mikulec, F. V.; Bawendi, M. G. The Band Edge Luminescence of Surface Modified CdSe Nanocrystallites: Probing the Luminescing State. *J. Chem. Phys.* **1997**, *106*, 9869–9882.
21. Bullen, C.; Mulvaney, P. The Effects of Chemisorption on the Luminescence of CdSe Quantum Dots. *Langmuir* **2006**, *22*, 3007–3013.
22. Munro, A. M.; Plante, I. J. L.; Ng, M. S.; Ginger, D. S. Quantitative Study of the Effects of Surface Ligand Concentration on CdSe Nanocrystal Photoluminescence. *J. Phys. Chem. C* **2007**, *111*, 6220–6227.
23. Kalyuzhny, G.; Murray, R. W. Ligand Effects on Optical Properties of CdSe Nanocrystals. *J. Phys. Chem. B* **2005**, *109*, 7012–7021.
24. Gaponik, N.; Talapin, D. V.; Rogach, A. L.; Hoppe, K.; Shevchenko, E. V.; Kornowski, A.; Eychmuller, A.; Weller, H. Thiol-Capping of CdTe Nanocrystals: An Alternative to Organometallic Synthetic Routes. *J. Phys. Chem. B* **2002**, *106*, 7177–7185.
25. Wuister, S. F.; de Mello Donegá, C.; Meijerink, A. Influence of Thiol Capping on the Exciton Luminescence and Decay Kinetics of CdTe and CdSe Quantum. *J. Phys. Chem. B* **2004**, *108*, 17393–17397.

26. Katari, J. E. B.; Colvin, V. L.; Alivisatos, A. P. X-Ray Photoelectron-Spectroscopy of CdSe Nanocrystals with Applications to Studies of the Nanocrystal Surface. *J. Phys. Chem.* **1994**, *98*, 4109–4117.
27. Becerra, L. R.; Murray, C. B.; Griffin, R. G.; Bawendi, M. G. Investigation of the Surface-Morphology of Capped CdSe Nanocrystallites by P-31 Nuclear-Magnetic-Resonance. *J. Chem. Phys.* **1994**, *100*, 3297–3300.
28. Gaunt, J. A.; Knight, A. E.; Windsor, S. A.; Chechik, V. Stability and Quantum Yield Effects of Small Molecule Additives on Solutions of Semiconductor Nanoparticles. *J. Colloid Interface Sci.* **2005**, *290*, 437–443.
29. Ji, X.; Copenhaver, D.; Sichmeller, C.; Peng, X. Ligand Bonding and Dynamics on Colloidal Nanocrystals at Room Temperature: The Case of Alkylamines on CdSe Nanocrystals. *J. Am. Chem. Soc.* **2008**, *130*, 5726–5735.
30. Jasieniak, J.; Mulvaney, P. From Cd-Rich to Se-Rich—the Manipulation of CdSe Nanocrystal Surface Stoichiometry. *J. Am. Chem. Soc.* **2007**, *129*, 2841–2848.
31. Schapotschnikow, P.; Pool, R.; Vlugt, T. J. H. Selective Adsorption of Alkyl Thiols on Gold in Different Geometries. *Comput. Phys. Commun.* **2007**, *177*, 154–157.
32. Pool, R.; Schapotschnikow, P.; Vlugt, T. J. H. Solvent Effects in the Adsorption of Alkyl Thiols on Gold Structures: A Molecular Simulation Study. *J. Phys. Chem. C* **2007**, *111*, 10201–10212.
33. Luedtke, W. D.; Landman, U. Structure and Thermodynamics of Self-Assembled Monolayers on Gold Nanocrystallites. *J. Phys. Chem. B* **1998**, *102*, 6566–6572.
34. Rabani, E. Structure and Electrostatic Properties of Passivated CdSe Nanocrystals. *J. Chem. Phys.* **2001**, *115*, 1493–1497.
35. Morgan, B. J.; Madden, P. A. A Molecular Dynamics Study of Structural Relaxation in Tetrahedrally Coordinated Nanocrystals. *Phys. Chem. Chem. Phys.* **2007**, *9*, 2355–2361.
36. Puzder, A.; Williamson, A. J.; Zaitseva, N.; Galli, G.; Manna, L.; Alivisatos, A. P. The Effect of Organic Ligand Binding on the Growth of CdSe Nanoparticles Probed by *Ab Initio* Calculations. *Nano Lett.* **2004**, *4*, 2361–2365.
37. Breus, V. V.; Heyes, C. D.; Nienhaus, G. U. Quenching of CdSe−ZnS Core−Shell Quantum Dot Luminescence by Water-Soluble Thiolated Ligands. *J. Phys. Chem. C* **2007**, *111*, 18589–18594.
38. Koole, R.; Luigjes, B.; Tachiya, M.; Pool, R.; Vlugt, T. J. H.; de Mello Donegá, C.; Meijerink, A.; Vanmaekelbergh, D. Differences in Cross-Link Chemistry between Rigid and Flexible Dithiol Molecules Revealed by Optical Studies of CdTe Quantum Dots. *J. Phys. Chem. C* **2007**, *111*, 11208–11215.
39. van Driel, A. F.; Allan, G.; Delerue, C.; Lodahl, P.; Vos, W. L.; Vanmaekelbergh, D. Frequency-Dependent Spontaneous Emission Rate from CdSe and CdTe Nanocrystals: Influence of Dark States. *Phys. Rev. Lett.* **2005**, *95*, 236804/1–236804/4.
40. Tolman, C. A. Steric Effects of Phosphorus Ligands in Organometallic Chemistry and Homogeneous Catalysis. *Chem. Rev.* **1977**, *77*, 313–348.
41. Breitlinger, D. K., Cadmium and Mercury. In *Comprehensive Coordination Chemistry II*; McCleverty, J. A., Meijer, T. J., Eds.; Elsevier: Amsterdam, 2004; Vol. 6; p 1253.
42. Aldana, J.; Lavelle, N.; Wang, Y. J.; Peng, X. G. Size-Dependent Dissociation Ph of Thiolate Ligands from Cadmium Chalcogenide Nanocrystals. *J. Am. Chem. Soc.* **2005**, *127*, 2496–2504.
43. Yu, W. W.; Qu, L.; Guo, W.; Peng, X. Experimental Determination of the Extinction Coefficient of CdTe, CdSe, and CdS Nanocrystals. *Chem. Mater.* **2003**, *15*, 2854–2860.